The Differential Imaging Features of Fat-Containing Tumors in the Peritoneal Cavity and Retroperitoneum: the Radiologic-Pathologic Correlation

Na-young Shin, MD[1]
Myeong-Jin Kim, MD[1]
Jae-Joon Chung, MD[1]
Yong-Eun Chung, MD[1]
Jin-Young Choi, MD[1]
Young-Nyun Park, MD[2]

There are a variety of fat-containing lesions that can arise in the intraperitoneal cavity and retroperitoneal space. Some of these fat-containing lesions, such as liposarcoma and retroperitoneal teratoma, have to be resected, although resection can be deferred for others, such as adrenal adenoma, myelolipoma, angiomyolipoma, ovarian teratoma, and lipoma, until the lesions become large or symptomatic. The third group tumors (i.e., mesenteric panniculitis and pseudolipoma of Glisson's capsule) require medical treatment or no treatment at all. Identifying factors such as whether the fat is macroscopic or microscopic within the lesion, the origin of the lesions, and the presence of combined calcification is important for narrowing the differential diagnosis. The development and widespread use of modern imaging modalities make identification of these factors easier so narrowing the differential diagnosis is possible. At the same time, lesions that do not require immediate treatment are being incidentally found at an increasing rate with these same imaging techniques. Thus, the questions about the treatment methods have become increasingly important. Classifying lesions in terms of the necessity of performing surgical treatment can provide important information to clinicians, and this is the one of a radiologist's key responsibilities.

Index terms:
Neoplasm, adipose tissue
Retroperitoneal space
Abdominal cavity
Tomography, spiral computed
Magnetic resonance (MR)

DOI:10.3348/kjr.2010.11.3.333

Korean J Radiol 2010;11:333-345
Received August 18, 2009; accepted after revision February 1, 2010.

Departments of [1]Radiology and [2]Pathology, Severance Hospital, Yonsei University School of Medicine, Seoul 120-752, Korea

Address reprint requests to:
Myeong-Jin Kim, MD, Department of Radiology, Severance Hospital, Yonsei University School of Medicine, 250 Seongsanno, Seodaemun-gu, Seoul 120-752, Korea.
Tel. (822) 2228-7400
Fax. (822) 393-3035
e-mail: kimnex@yuhs.ac

There are a variety of fat-containing lesions that can arise in the intraperitoneal cavity and retroperitoneal space (Table 1). Many authors use the organ of origin, the location of the fat-containing lesions or their malignancy to classify these lesions. With the development and wide-spread use of modern imaging modalities, incidental lesions that do not require immediate treatment are being detected increasingly. Therefore, the radiologist's role in differentiating lesions that require surgical therapy from those that do not is becoming more important. To do this, meticulous evaluation of fat-containing lesions for various characteristic features is essential to help avoid unnecessary surgical treatments.

Fat Seen on Imaging

On ultrasound (US) images, fat tissues usually appear hyperechoic, although there are exceptions. On computed tomography (CT), fat appears to have low attenuation with a range of −10 to −100 Hounsfield units (HUs). If the proportion of fat within a voxel is small, then the mean CT number will increase and fat may be difficult to reliably identify (1). Magnetic resonance (MR) imaging is more sensitive for detecting microscopic fat than CT or US. Fat appears hyperintense on the T1-weighted images and it appears intermediately intense to hyperintense on the T2-weighted fast spin-echo and gradient-echo images. MR imaging techniques use the difference of the

resonance frequencies of water and fat protons, such as in-phase/opposed-phase chemical shift imaging and the frequency-selective fat suppression techniques, and this can help identify fat more reliably (2).

Neoplasm Indicated for Removal

Liposarcoma

Liposarcomas are the most common primary retroperitoneal malignant neoplasm. They may also arise in the mesentery or peritoneum. Liposarcomas are histologically subdivided into five main subgroups in the order of increasing malignancy: 1) well-differentiated, 2) myxoid, 3) dedifferentiated 4) round cell and 5) pleomorphic liposarcoma (5) (Table 2). The CT and MR imaging appearances vary depending on the histologic subtype and the tumor components. For liposarcomas, surgical resection that is usually combined with the adjacent kidney is necessary, but complete surgical removal may be difficult and recurrence is common (3). The histologic subtype and the margin of the resection are prognostic factors for survival for patients with primary retroperitoneal liposarcoma (4). Radiologists play an important role not only in making the preoperative diagnosis, but also in correctly assessing the extent of the tumor.

Well-differentiated liposarcomas resemble lipomas, although liposarcomas tend to be larger and have dense collagen bands. Atypical hyperchromatic cells with angular nuclei and lipoblasts can also be seen (5). Well-differentiated liposarcomas may be sub-classified into three subtypes: 1) adipocytic (or lipoma-like) (Fig. 1), 2) sclerosing, and 3) inflammatory. The lipoma-like subtype shows low attenuation on CT images and high signal intensity on the T1- and T2-weighted MR images, similar to subcutaneous fat. The fibrous septa may be thicker, more irregular or more nodular than those seen in lipomas (2). The sclerosing subtype shows CT attenuation or an MR signal intensity that approximates the characteristics of muscle. The septa within the lipoma-like components and sclerosing components can be homogeneously enhanced on contrast-enhanced CT and on the fat-suppressed T1-weighted MR images after administration of gadolinium chelate (6). The inflammatory subtype, which is relatively rare and has the histological feature of an extensive lymphoplasmacytic infiltration, appears as a fibro-fatty mass on CT. The inflammatory component may show a homogeneous hyperintense signal on the T2-weighted MR images (7).

Table 1. Fat-Containing Lesions in Intraperitoneal Cavity and Retroperitoneal Space

	Intraperitoneal Cavity	Retroperitoneal Space	Characteristic Features
Indicated for removal	Liposarcoma	Liposarcoma	Lobulated or ill-marginated fatty mass with soft tissue component
		Retroperitoneal teratoma	Encapsulated round or ovoid fatty mass with dense calcification. It is found in retroperitoneum
		Immature teratoma	Coarse calcification, dominant soft tissue component and smaller fat foci
		Renal cell carcinoma	Predominant hypervascular renal mass that may be associated with macroscopic fat and calcification
Indicated for removal only when symptomatic or large		Adrenal adenoma	Microscopic fat in mass and mass originates from adrenal gland
		Myelolipoma	Macroscopic fat in mass and mass originates from adrenal gland
		Angiomyolipoma	Macroscopic fat in mass. Mass originates from kidney
		Mature cystic teratoma of ovary	Fat-fluid level +/− calcification in well-encapsulated mass. Mass originates from ovary
	Lipoma	Lipoma	Homogeneous, fat attenuated mass +/− thin fibrous septa
Miscellaneous	Mesenteric panniculitis		Fatty mass surrounding superior mesenteric vessels without vessel narrowing
		Pseudolipoma of Glisson's capsule	Small nodule on liver surface and nodule shows fat attenuation or signal intensity on liver surface

The myxoid and round cell liposarcomas represent a morphologic continuum, and the histologic grading is based on the extent of the round cell component (4). Myxoid liposarcoma is the most common subtype of liposarcomas. Myxoid liposarcoma has a prominent myxoid stroma with or without delicate arborizing vasculature (4). The myxoid components show less attenuation than that of muscle on CT scans, with similar signal intensity to that of water, and they are hypointense compared with muscle on the T1-weighted images and hyperintense compared with fat on

Table 2. Subtypes of Liposarcoma

Liposarcoma Subtypes		Clinicopathological Feature	Imaging Findings
Well-differentiated	Adipocytic (or lipoma-like)	Resemble lipomas Larger size Dense collagen bands	Lipoma-like component - Similar to subcutaneous fat - Fibrous septa: thicker, more irregular or more nodular than those seen in lipomas
	Sclerosing	Collagenous fibrous tissue	Sclerosing component - Similar to muscle - Homogeneous contrast enhancement
	Inflammatory	An extensive lymphoplasmacytic infiltrate	Well-defined non-lipomatous masses juxtaposed with fatty tumor Inflammatory component - Homogeneous signal intensity on T2 weighted image
Myxoid		Uniform round-to-oval-shaped primitive nonlipogenic mesenchymal cells Prominent myxoid stroma +/− delicate arborizing vasculature	Myxoid component - Mimics a cystic lesion on precontrast CT or MRI - Gradual reticular enhancement
Round cell		More round cell components Less myxoid matrix and capillary networks	Nonspecific soft-tissue masses
Pleomorphic		Pleomorphic spindle cells and giant cells Sheets of pleomorphic lipoblasts	Nonspecific soft-tissue masses
Dedifferentiated		Well-differentiated liposarcoma juxtaposed to pleomorphic sarcoma	Well-defined non-lipomatous masses juxtaposed with fatty tumor Non-lipomatous mass - Homogeneous signal intensity on T2 weighted image

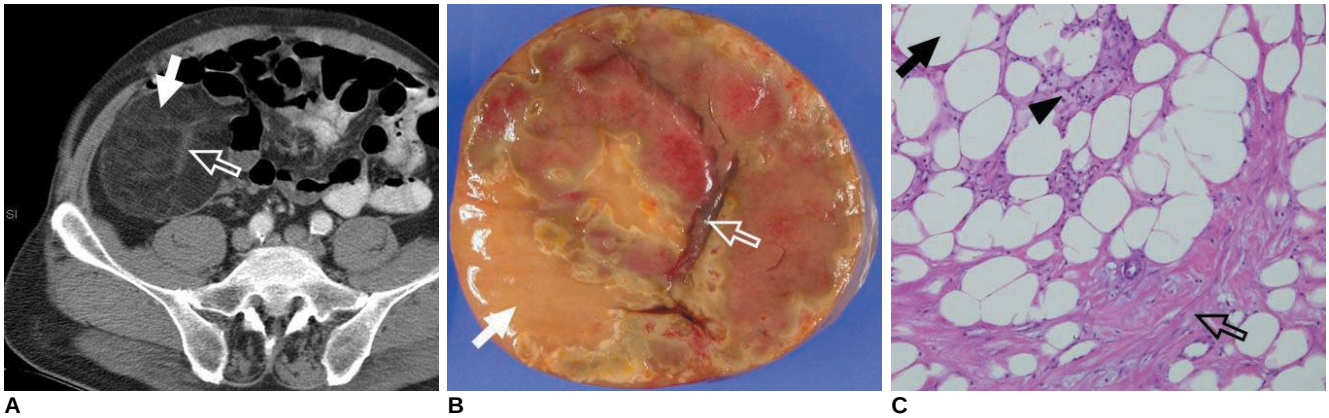

A **B** **C**

Fig. 1. 64-year-old man with pathologically proven lipoma-like, well-differentiated liposarcoma.
A. Contrast-enhanced CT scan shows well-defined, heterogeneous mass with predominant fat attenuation (arrow). Slightly coarse and thickened fibrous septa (open arrow) with enhancement suggest lipoma-like, well-differentiated liposarcoma.
B. Photograph of gross pathologic specimen shows homogeneously yellow adipose tissue (arrow) and septal structure (open arrow).
C. Photomicrograph (Hematoxylin & Eosin staining, × 200) demonstrates mature adipocytes (arrow) that exhibit variations of cell size and multi-vacuolated lipoblasts (arrowhead) with fibrous septa (open arrow).

the T2-weighted spin-echo images. The fibrous septa within the myxoid components show low signal intensity on the T2-weighted MR images (6) (Fig. 2). Before contrast enhancement, the myxoid components show CT attenuation and MR signal intensity similar to that of fluid. Lacy, linear or amorphous regions of high signal intensity can be noted on the T1-weighted images and intermediate signal intensity can noted on the T2-weighted images, which represent intratumoral fat, and these features permit making the correct diagnosis. Recognition of chemical shift artifacts between the water- and fat-based components also facilitates an accurate diagnosis. After contrast enhancement, gradual reticular enhancement may be seen within the myxoid components. Although myxoid liposarcomas may appear to be cystic lesions before contrast enhancement, they can be correctly characterized as solid lesions on the contrast-enhanced images (2).

Round cell liposarcoma contains more round cell

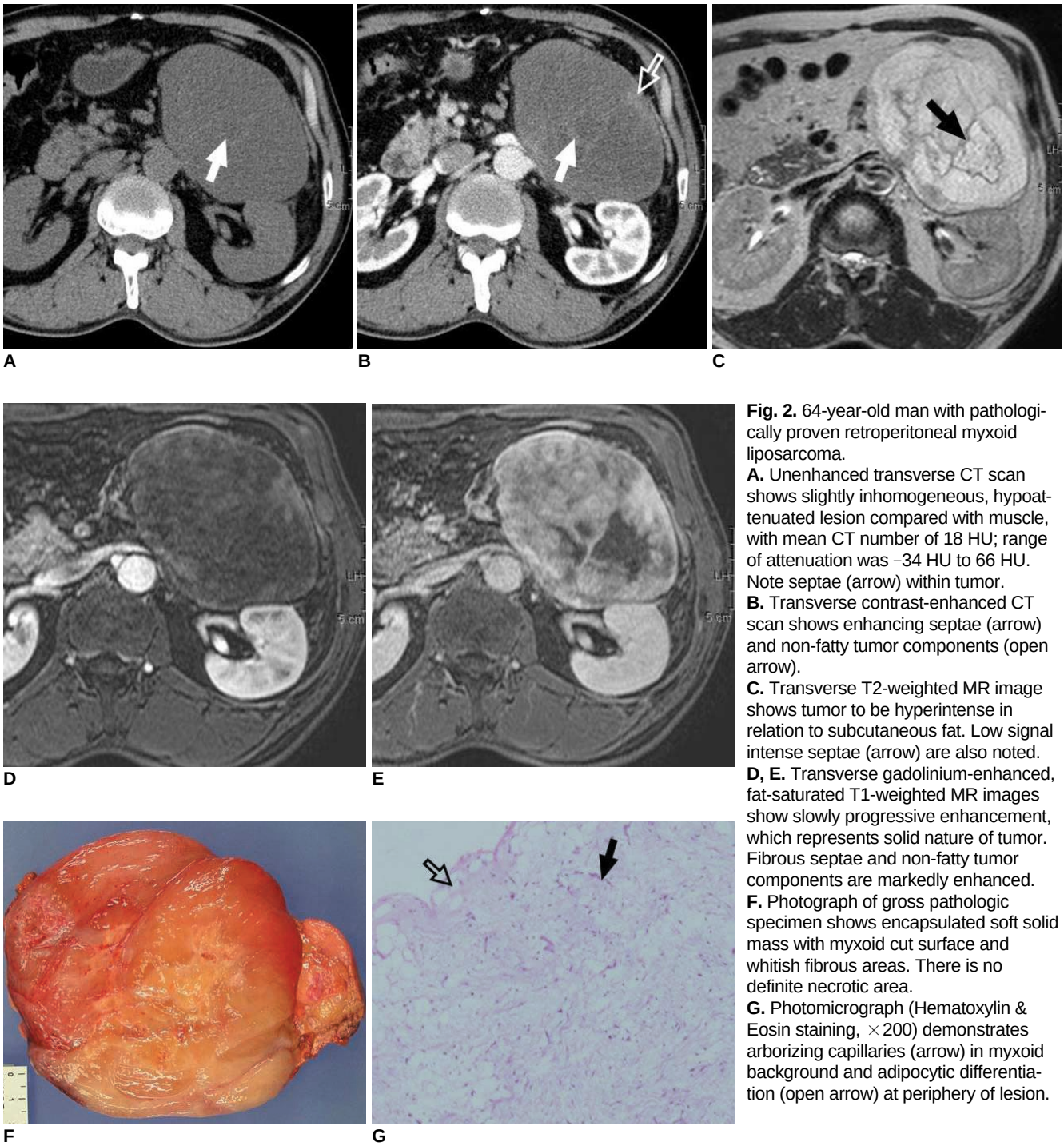

Fig. 2. 64-year-old man with pathologically proven retroperitoneal myxoid liposarcoma.
A. Unenhanced transverse CT scan shows slightly inhomogeneous, hypoattenuated lesion compared with muscle, with mean CT number of 18 HU; range of attenuation was −34 HU to 66 HU. Note septae (arrow) within tumor.
B. Transverse contrast-enhanced CT scan shows enhancing septae (arrow) and non-fatty tumor components (open arrow).
C. Transverse T2-weighted MR image shows tumor to be hyperintense in relation to subcutaneous fat. Low signal intense septae (arrow) are also noted.
D, E. Transverse gadolinium-enhanced, fat-saturated T1-weighted MR images show slowly progressive enhancement, which represents solid nature of tumor. Fibrous septae and non-fatty tumor components are markedly enhanced.
F. Photograph of gross pathologic specimen shows encapsulated soft solid mass with myxoid cut surface and whitish fibrous areas. There is no definite necrotic area.
G. Photomicrograph (Hematoxylin & Eosin staining, × 200) demonstrates arborizing capillaries (arrow) in myxoid background and adipocytic differentiation (open arrow) at periphery of lesion.

components and less myxoid matrix and capillary networks than myxoid liposarcomas, and round cell liposarcoma is considered to be a high-grade sarcoma with a higher likelihood of metastasis and death (8). Round-cell liposarcoma shows CT attenuation approximating that of muscle. On the contrast-enhanced CT images, round cell liposarcoma has heterogeneous enhancement with irregular hypoattenuation (Fig. 3). On the MR images, round-cell liposarcoma is seen as a soft tissue mass that is hypointense relative to muscle on the T1-weighted images, it is slightly hyperintense relative to muscle on the T2-weighted images and it shows strong enhancement on the contrast-enhanced images. These non-fatty tumors can be accompanied with necrosis or hemorrhage (9). These characteristics are usually indistinguishable from those of other malignant soft-tissue masses.

Pleomorphic liposarcoma is the least common subtype; it is a high-grade, very aggressive tumor. On microscopy, pleomorphic liposarcoma is characterized by pleomorphic spindle cells and giant cells, as well as sheets of pleomorphic lipoblasts (4). Pleomorphic liposarcoma shows CT attenuation approximating that of muscle (6). Pleomorphic liposarcoma exhibits ill-defined and soft-tissue signal intensity equal to that of muscle on the T1-weighted spin-

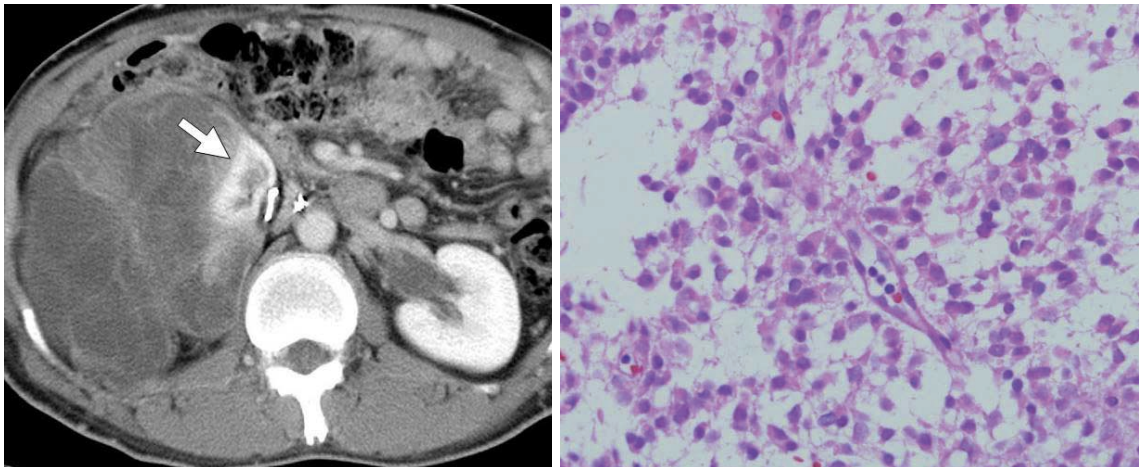

Fig. 3. 45-year-old man with pathologically proven myxoid/round cell liposarcoma.
A. Axial contrast-enhanced CT scan shows heterogeneous non-fatty mass displacing right kidney superiorly and medially (arrow) with areas of hypoattenuation that represent myxoid components.
B. Photomicrograph (Hematoxylin & Eosin staining, × 200) demonstrates undifferentiated round cell morphology with myxoid component.

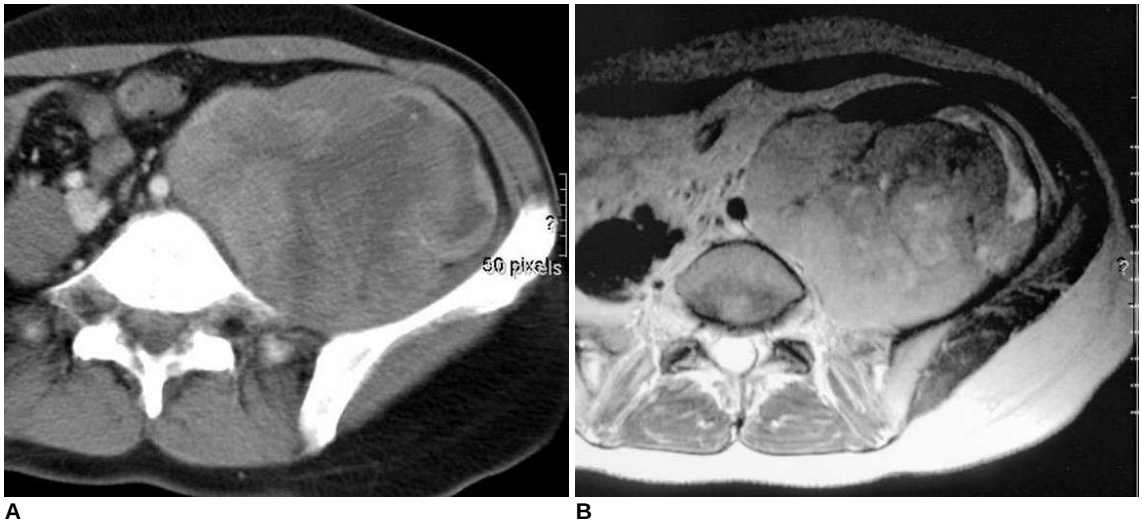

Fig. 4. 30-year-old woman with pathologically proven pleomorphic liposarcoma.
A. Axial contrast-enhanced CT scan shows soft tissue tumor with heterogeneous enhancement.
B. Axial T2-weighted MR image shows heterogeneous, high signal intense tumor. Signal intensity is similar to or slightly lower than that of subcutaneous fat.

echo MR images and this is equal to that of fat on the T2-weighted spin-echo MR images without characteristic manifestations (9) (Fig. 4). There are no characteristic signals on MRI, so it is very difficult to differentiate this tumor from other retroperitoneal soft tissue tumors.

Dedifferentiated liposarcoma is most commonly located in the retroperitoneum, and this is defined as a neoplasm with a well-differentiated liposarcoma juxtaposed to pleomorphic sarcoma. On the CT and MR images, dedifferentiated liposarcoma is seen as well-defined non-lipomatous masses juxtaposed with fatty tumor (10). On the T1-weighted MR images, the signals are hypointense relative to the muscle signals, whereas on the T2-weighted MR images, the tumors show heterogeneous hyperintense signals relative to the muscle intensities (Fig. 5). The heterogeneity on T2-weighted images may be a clue for differentiation between the inflammatory subtype of well-differentiated liposarcoma and dedifferentiated liposarcoma (7). The tumor extent should be defined with caution as the fat components of the tumor could easily be mistaken for adjacent normal fat structures, and missed tumor components could be left after surgical resection (Fig. 6). According to Tateishi et al. (10), the presence of calcification or ossification and the first recurrence after a mean of 13 months, as identified by CT and MRI studies, are significant adverse prognostic factors for primary dedifferentiated liposarcoma of the retroperitoneum.

Retroperitoneal Teratoma

Primary retroperitoneal teratomas account for 1–11% of all retroperitoneal neoplasms (11). These tumors are very rare in adults, but there is a 26% chance of malignant change (12). Retroperitoneal teratomas are often located near the upper pole of the kidney with preponderance on the left side. They have been confused with ovarian and adrenal tumors such as adrenal myelolipomas, as well as with a variety of renal and retroperitoneal masses including Wilms' tumors, renal cysts, retroperitoneal fibromas, sarcomas, hemangiomas and enlarged lymph nodes (12). The most characteristic radiologic findings of mature teratoma of the retroperitoneum are a complex mass that contains a well-circumscribed fluid component of variable volume, adipose tissue and/or sebum in the form of a fat-fluid level, and calcification in either a congealed or linear strand pattern (13) (Fig. 6). Although the presence of a fat-fluid level is highly specific for a teratoma, a fat-fluid level has also been described in a case of well-differentiated liposarcoma of the retroperitoneum (14). Thus, surgical resection remains the mainstay of therapy and this is required for making the definitive diagnosis (11).

Indicated for Removal Only When Symptomatic or Large

Adrenal Adenoma

Adrenal adenoma is common tumor that is usually detected incidentally, and it has shown a prevalence of 3%

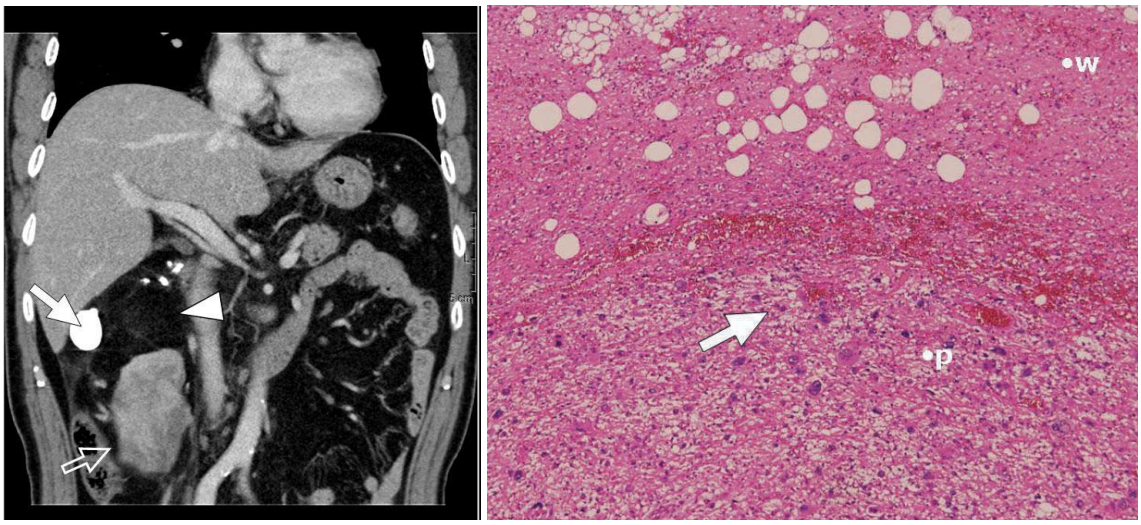

Fig. 5. 56-year-old woman with pathologically proven dedifferentiated liposarcoma.
A. Coronal contrast-enhanced CT image shows non-lipomatous mass (open arrow) abruptly juxtaposed with fatty tumor (arrowhead). Mass was diagnosed as retroperitoneal soft tissue sarcoma without considering fat component as part of tumor and incomplete resection was done, which failed to remove neoplastic fat component. Considerable amount of well-differentiated liposarcoma was left. Metaplastic ossification (arrow), which is adverse prognostic factor, is also noted.
B. Photomicrograph (Hematoxylin & Eosin staining, × 40) demonstrates abrupt transition from well-differentiated liposarcoma (w) to hypercellular high-grade sarcoma (p). Pleomorphic cells (arrow) are demonstrated in dedifferentiated area.

in a previous autopsy series (15). Although they are usually nonfunctional, hyperfunctional adenomas can also occur and they can account for endocrine disorders such as Cushing syndrome and Conn syndrome. On CT scans, adrenal adenomas appear as small, well-defined homogeneous masses that are typically hypo-attenuating relative to the liver. A cutoff of 10 HU on the unenhanced CT scan and a relative percentage of washout of more than 50% on the delayed study can be used for detecting adenomas (2, 16). Microscopic fat within adrenal adenomas appears as signal loss on the opposed-phase MR images when compared with that of the in-phase MR images (Fig. 7). These chemical shift MR images are more sensitive for detecting adrenal adenomas than CT scans. If there is evidence of autonomous adrenal steroid production, then surgery (either open or laparoscopic) is indicated, whenever possible, to remove the tumor and to correct any excess steroid hormone. Therapy can be deferred when the tumor is an incidental finding, it is small (< 3 or 4 cm) and it has the above-mentioned typical radiographic features of adrenal adenoma (2, 16).

Angiomyolipoma

Angiomyolipoma (AML) is the most common benign tumor of the kidney and it is composed of varying amounts of thick-walled dysplastic or dysmorphic blood vessels, smooth muscle and mature adipose elements derived from perivascular epithelioid cells (17). AML is seen in two distinct clinical settings: 1) sporadic or in association with tuberous sclerosis. The sporadic form accounts for approximately 80–90% of the cases of AML and it is most commonly found in middle-aged women (18). Although hemorrhage is a frequent complication, necrosis and calcification are rare. AML can usually be diagnosed in a

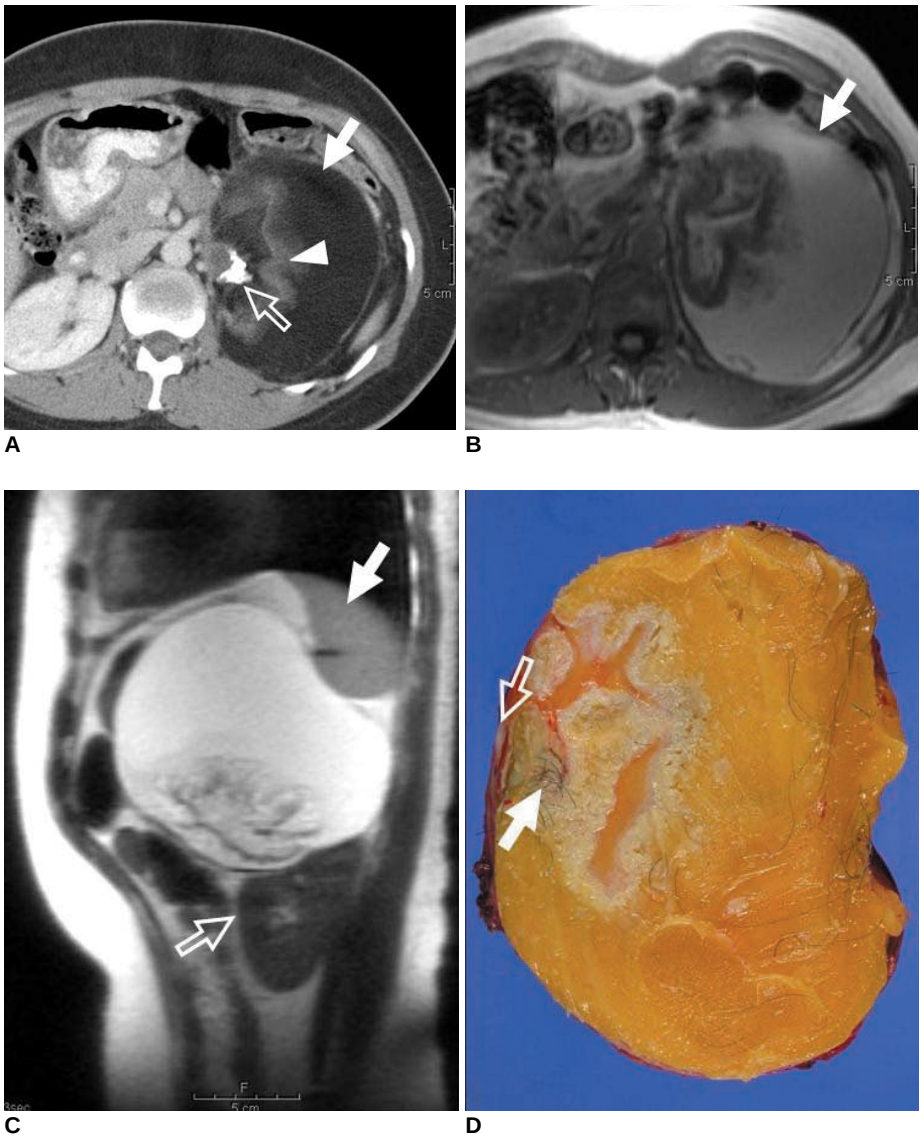

Fig. 6. 33-year-old woman with periadrenal mature teratoma.
A. Transverse contrast-enhanced CT scan shows well encapsulated cystic mass with fat (arrow) and calcification (open arrow). Isodense, feathery appearance (arrowhead) representing hair is noted.
B. Macroscopic fat component (arrow) in cystic mass shows high signal intensity on T1-weighted gradient-echo MR image.
C. Sagittal T1-weighted gradient MR image shows displaced spleen (arrow) and left kidney (open arrow).
D. Photograph of gross pathologic specimen shows yellowish butter-like keratinous material with hair follicles (arrow) and calcified material (open arrow).

straightforward manner on the US, CT or MR images by identifying the intratumoral fat component. On sonography, AMLs appear hyperechogenic with acoustic shadowing. On CT, these lesions typically appear as well-defined, cortical masses of predominantly fat attenuation with heterogeneous soft-tissue attenuation interspersed throughout. Intratumoral fat is the component that has been best characterized on the MR images. This fat appears as high signal intensity on the T1-weighted MR imaging with loss of signal intensity on the fat-suppressed images (Fig. 8). The chemical shift misregistration artifact on spin-echo images and the India ink artifact due to chemical shift interference between the fat and water interface are also used for diagnosing AML (19).

Because there have been rare reports of renal cell carcinomas (RCC) with fat attenuation (less than –20 HU) on CT and because several renal lesions other than AML may contain fat, such as liposarcoma, lipoma, myolipoma and Wilms tumor in children, fat is not diagnostic proof of AML. AML is also a challenge to diagnose because AML with minimal fat mimics RCC. AMLs can require emergency treatment (embolization or surgery) if life-threatening bleeding occurs, but they do not necessarily require surgery (20). Surgical resection is necessary for malignant lesions such as RCC or retroperitoneal liposarcoma. Therefore, making an accurate diagnosis of AML is important to prevent unnecessary surgery.

The fat components within RCC can be caused by engulfment of the perirenal or renal sinus fat into the tumor, intratumoral bone metaplasia with fatty marrow elements or the presence of cholesterol necrosis that is misinterpreted as fat (21). As most RCCs with fat densities show calcification, fat-containing lesions with calcification favors a diagnosis of RCC rather than AML and this should be recommended for surgery (21).

Homogeneous tumor enhancement and prolonged enhancement patterns on biphasic helical CT may be useful for differentiating AML with minimal fat from RCC (22).

Large exophytic AMLs and well-differentiated retroperitoneal liposarcomas can have similar appearances on imaging studies. A careful evaluation for a sharp defect in the renal parenchyma and the presence of enlarged vessels

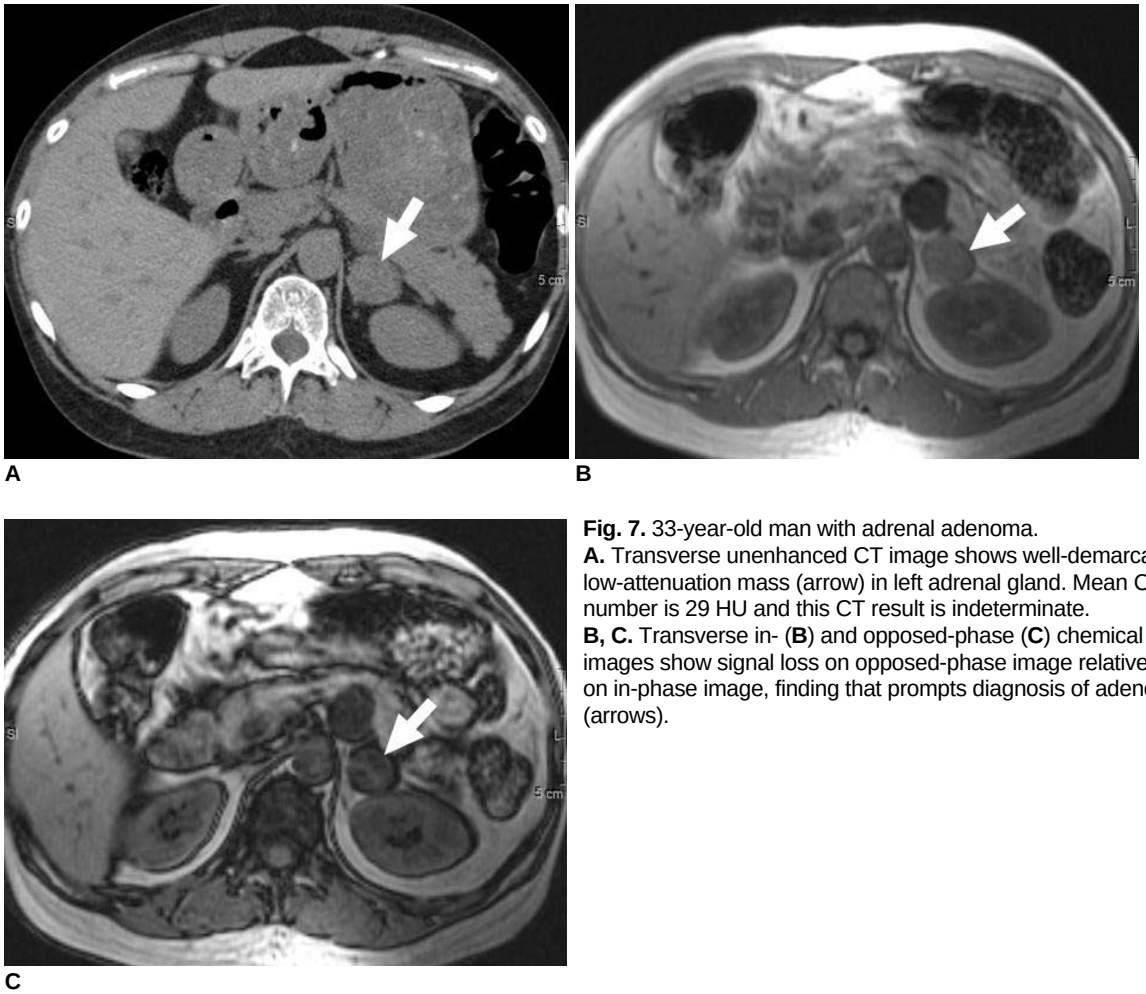

Fig. 7. 33-year-old man with adrenal adenoma.
A. Transverse unenhanced CT image shows well-demarcated, low-attenuation mass (arrow) in left adrenal gland. Mean CT number is 29 HU and this CT result is indeterminate.
B, C. Transverse in- (**B**) and opposed-phase (**C**) chemical shift MR images show signal loss on opposed-phase image relative to that on in-phase image, finding that prompts diagnosis of adenoma (arrows).

and associated AMLs should enable accurately differentiating these lesions from primary retroperitoneal fatty tumors in almost all cases (3). In contrast, because liposarcoma arises in the retroperitoneal fat, it does not cause a defect in the renal parenchyma, and the interface of the lesion with the kidney is smooth. AMLs usually contain enlarged vessels

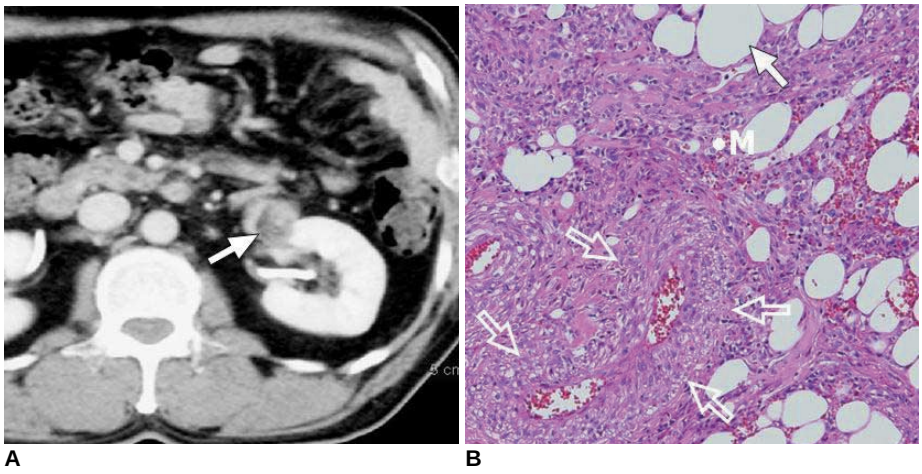

A B

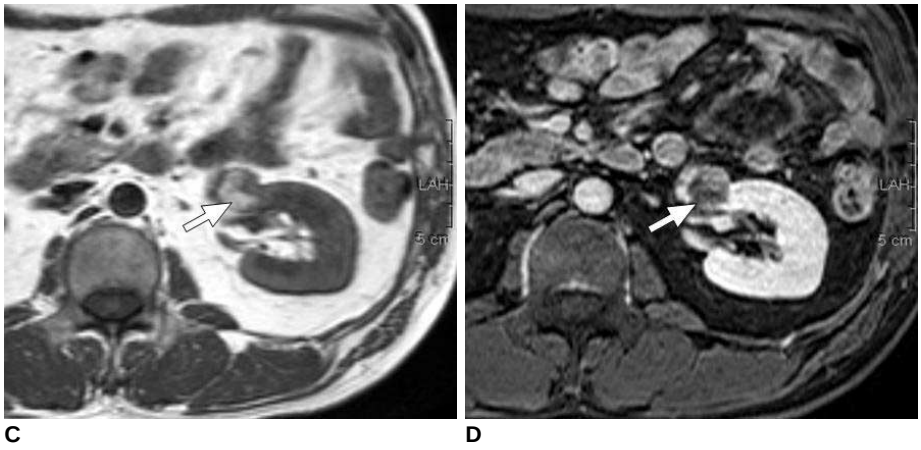

C D

Fig. 8. 48-year-old man with angiomyolipoma.
A. Contrast-enhanced CT scan shows well-defined, cortically based mass with focal areas of fat attenuation (arrow).
B. Photomicrograph (Hematoxylin & Eosin staining, × 100) shows adipocytes (arrow), smooth muscle cells (M) and thick-walled vessels (open arrows).
C, D. These (arrows) appear hyperintense on T1-weighted MR image (**C**) with signal loss on gadolinium-enhanced fat saturation T1-weighted image (**D**).

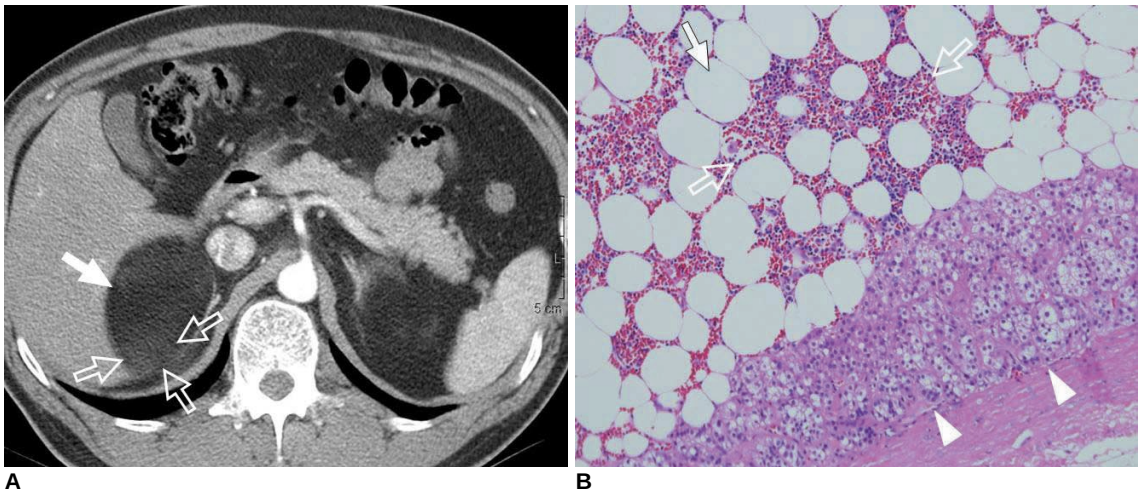

A B

Fig. 9. 44-year-old man with adrenal myelolipoma.
A. Transverse contrast-enhanced CT scan shows well-defined fatty mass (arrow) in adrenal area interspersed with enhancing soft tissue components (open arrows).
B. Photomicrograph (Hematoxylin & Eosin staining, × 100) shows areas of myeloid and erythroid precursor cells (open arrows) among adipocytes (arrow) within mass. Adrenal cortical cells (arrowheads) adjacent to lesion are identified.

that can be seen with contrast-enhanced CT. In comparison, well-differentiated liposarcomas are relatively avascular. The presence of other fatty lesions in the ipsilateral or contralateral kidney, independent of the dominate lesion, is a strong indicator that the tumor in question is an AML (3).

Myelolipoma

Myelolipoma is an uncommon tumor and it is composed of a variable mixture of mature fat and hematopoietic elements that resembles bone marrow (23). Although most myelolipomas have been found in the adrenal gland, extra-adrenal (most often in the retroperitoneum) myelolipomas also reported (24). Myelolipoma may be accompanied by acute hemorrhage and calcification, which can complicate making the image-based diagnosis. On US, myelolipoma often shows heterogeneous echogenicity due to its nonuniform architecture. Myelolipoma is typically seen as a hyperechogenic mass with more hypoechoic regions in the predominantly myeloid components (25). CT frequently demonstrates large amounts of fat with areas of interspersed higher-attenuation tissue. On MR imaging, due to the nonuniform mixture fat and marrow components, the fatty component is usually hyperintense on the T1-weighted images and heterogeneously hyperintense on the T2-weighted images (2). Frequency-selective fat-suppressed MR imaging allows confirmation of the diagnosis of myelolipoma by demonstrating signal loss. Opposed-phase imaging should demonstrate low signal intensity in the voxels containing both fat and water tissue (24) (Fig. 9). Surgical excision is not necessary unless the diagnosis is in question or the lesion is symptomatic. Patients with large asymptomatic tumors over 10 cm in size should also be surgically treated because there is a small, but distinct risk of developing abdominal pain or life-threatening shock from spontaneous hemorrhage, and particularly in the case of large myelolipomas because hemorrhage often occur in these tumors (26).

It is difficult to differentiate giant adrenal or extra-adrenal myelolipomas from other fat-containing soft-tissue masses such as lipoma, liposarcoma, myolipoma, teratoma and an exophytic AML of the kidney. Therefore, percutaneous needle biopsy is often needed to confirm the diagno-

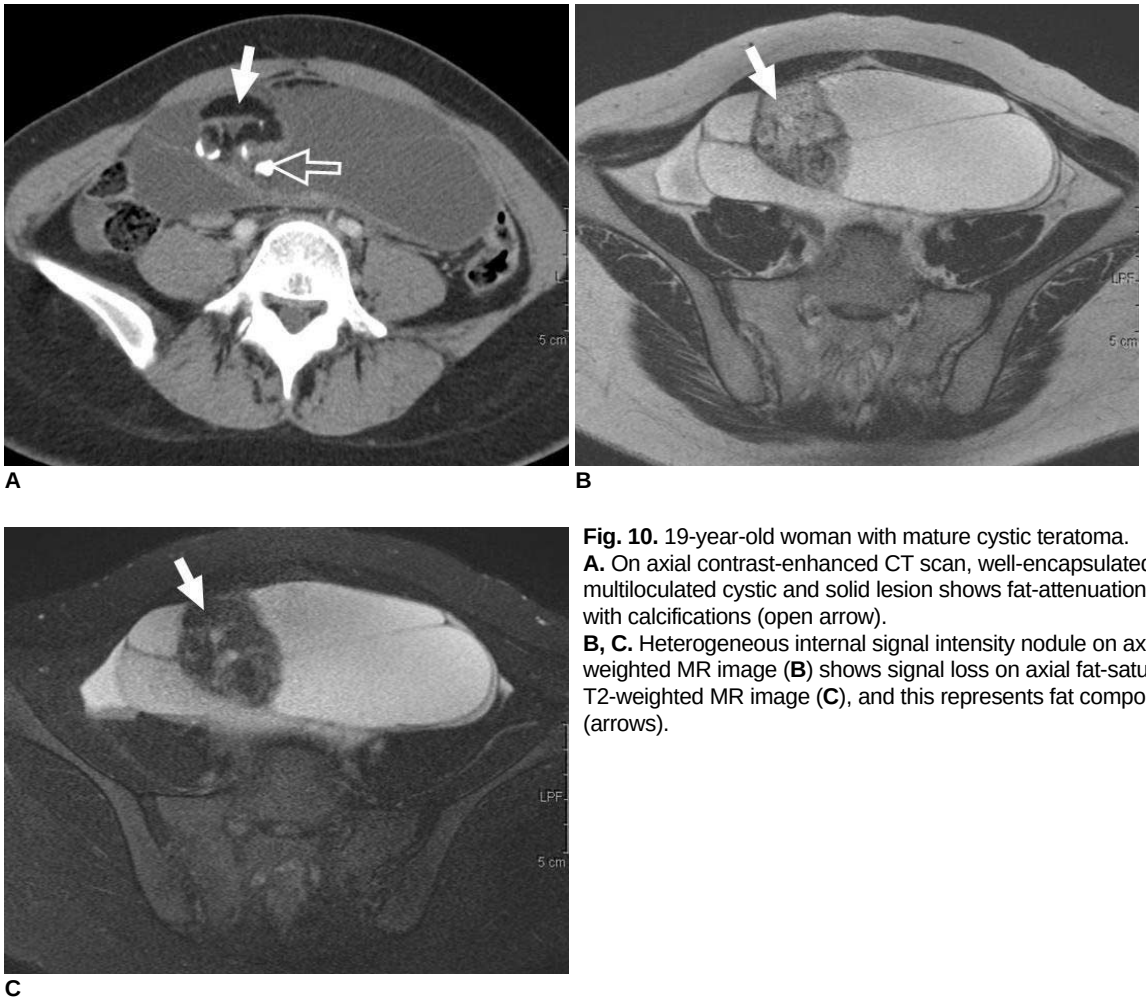

Fig. 10. 19-year-old woman with mature cystic teratoma.
A. On axial contrast-enhanced CT scan, well-encapsulated, multiloculated cystic and solid lesion shows fat-attenuation (arrow) with calcifications (open arrow).
B, C. Heterogeneous internal signal intensity nodule on axial T2-weighted MR image (**B**) shows signal loss on axial fat-saturated T2-weighted MR image (**C**), and this represents fat component (arrows).

sis (27).

Ovarian Teratoma

Ovarian teratomas are the most common germ cell neoplasm. Mature cystic teratomas (also known as dermoid cysts) are the most common of these tumors, and mature cystic teratomas are cystic tumors composed of well-differentiated derivations from at least two of the three germ cell layers (ectoderm, mesoderm and endoderm). Adipose tissue is seen in 67–75% of the cases, and teeth are present in 31% (28). Immature teratomas that demonstrate clinically malignant behavior have immature or embryonic tissues. In monodermal teratomas, one of these tissue types predominates, such as struma ovarii (thyroid tissue), ovarian carcinoid tumor (neuro-ectodermal tissue), and tumor with neural differentiation.

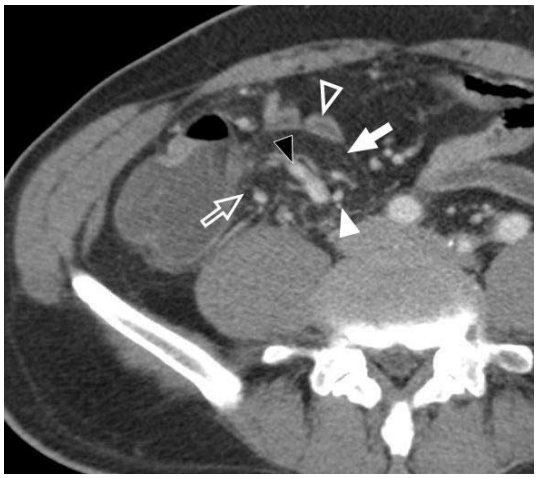

Fig. 11. 70-year-old man with acute pathologically proven mesenteric panniculitis. Axial contrast-enhanced CT scan shows ill-defined, inhomogeneous fatty mass with hyperdense peripheral stripe (arrow). Mesenteric vessels (black arrowhead) with no distortion and lymph nodes (white arrowhead) are engulfed by fatty halos (open arrow). Note smooth displacement in adjacent small bowel loops (white open arrowhead).

Although mature cystic teratomas show various appearances on US, most can be characterized by the presence of echogenic sebaceous material and calcification. When there is fat attenuation within a cyst on CT, with or without calcification in the wall, it is diagnostic of mature cystic teratoma. On MR imaging, the fat-suppressed images can specifically identify the sebaceous component (Fig. 10). The typical US appearances are heterogeneous, partially solid lesions, usually with scattered calcifications, although these are non-specific for immature teratomas. Both CT and MR imaging show the characteristic appearance of immature teratoma as a large, irregular solid component containing coarse calcifications. Small foci of fat also help characterize these tumors, and hemorrhage is often present. The US features of struma ovarii are also nonspecific, but a complex appearance with multiple cystic and solid areas may be seen. The cystic spaces demonstrate both high and low signal intensity on the T1- and T2-weighted images. On both the T1- and T2-weighted images, some of the cystic spaces may demonstrate low signal intensity due to the thick, gelatinous colloid of the struma. Fat is not evident in these lesions (28).

Mature cystic teratoma can be associated with complications from torsion, rupture, and malignant degeneration. Although most mature cystic teratomas are asymptomatic, the minority of patients with this malady present with abdominal pain or other nonspecific symptoms. Because of the slow growth of dermoid cysts (1.8 mm per year),

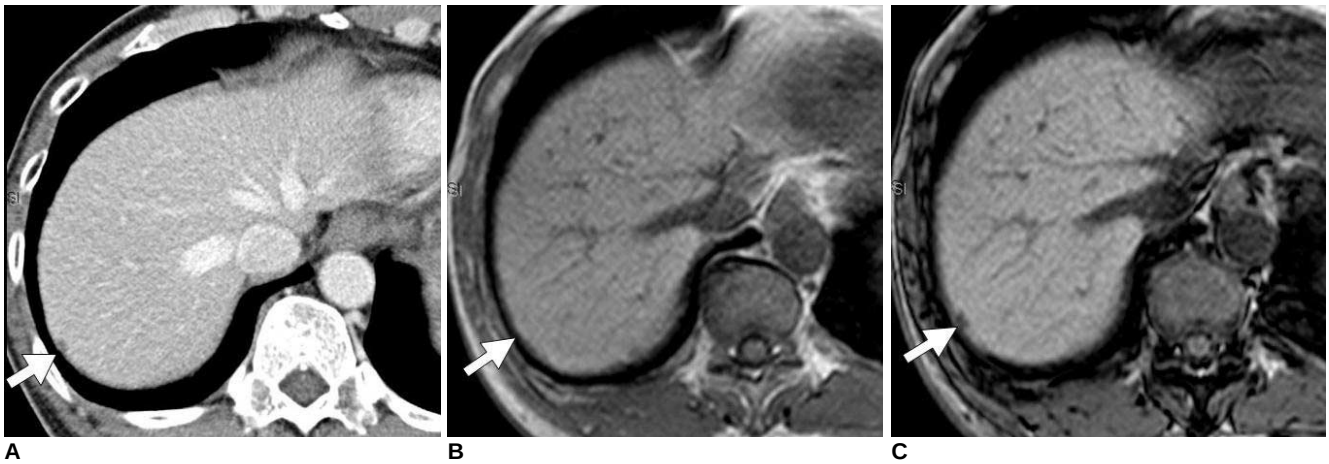

A **B** **C**

Fig. 12. 60-year-old man with pseudolipoma of Glisson's capsule.
A. Axial contrast-enhanced CT scan shows well-demarcated, hypoattenuating nodule (arrow) in subcapsular region of right hepatic lobe with mean CT number of 50 HU. Lesion is not differentiated from metastatic nodule.
B, C. Nodule appears with high signal intensity on in-phase MR image (**B**) and nodule (arrows) has signal loss on opposed-phase image (**C**). These findings are suggestive of fat-containing pseudolipoma of Glisson's capsule.

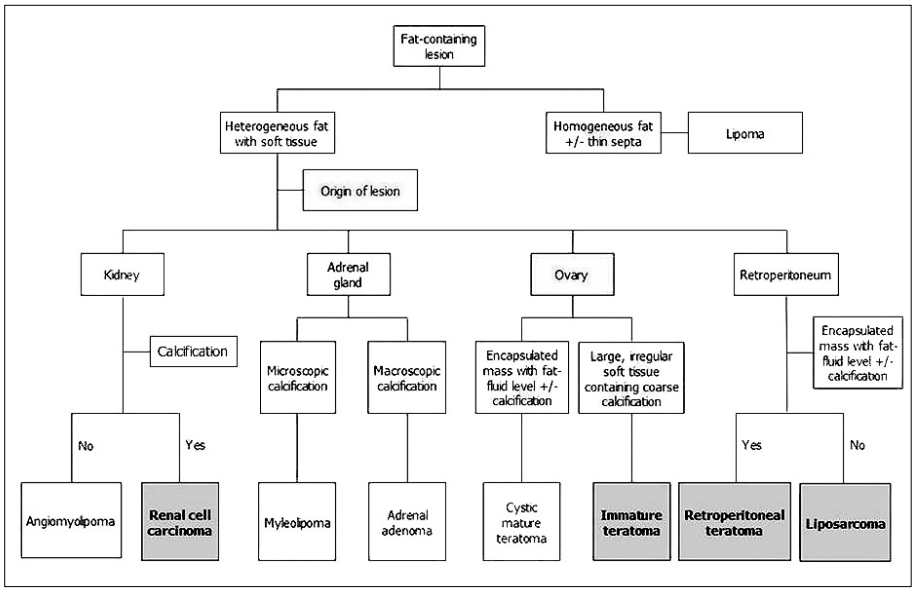

Fig. 13. Algorithm to differentiate fat-containing lesions in intraperitoneal cavity and retroperitoneal space. Bold letters indicate lesions that require surgical resection.

nonsurgical management for asymptomatic, noncomplicated lesions less than 6 cm in diameter is recommended while immature teratomas require surgical treatment with or without chemotherapy (29, 30). Mature cystic teratomas requiring removal can be treated according to age, the desire to maintain fertility or the presence of another pelvic pathology rather than their size or bilaterality, and simple cystectomy is favored for younger patients who have lower gravidity and parity to preserve as much ovarian tissue as possible (28, 31).

Miscellaneous

Mesenteric Panniculitis

Mesenteric panniculitis is a rare idiopathic disorder. It typically involves the adipose tissue of the bowel mesentery by chronic, nonspecific inflammation. When symptomatic, a palpable abdominal mass and systemic manifestations can occur, including abdominal pain, pyrexia, weight loss and bowel disturbances of variable duration. On the CT images, mesenteric panniculitis can appear as a solitary ill-defined mass of inhomogeneous fatty tissue at the root of the jejunal mesentery (Fig. 11). It is characterized by envelopment of the superior mesenteric vessels without vascular narrowing, and there is displacement of the adjacent bowel loops and well-defined soft tissue nodules (lymph nodes) scattered throughout the mass. A distinctive, hypo-attenuating fatty halo that typically surrounds the nodules and vessels is suggestive of mesenteric panniculitis. Yet this is not specific because it can be found in other entities such as lymphoma. A hyperattenuating stripe partially surrounding the mass is also suggestive of the diagnosis of mesenteric panniculitis (32). There is no specific treatment. Medical treatment may consist of therapy with anti-inflammatory or immunosuppressive agents. According to some authors, steroid treatment may decrease the amount of inflammation and improve the course of the disease (33). Partial resection is recommended when the advanced inflammatory changes become irreversible, and especially in the case of bowel obstruction (34).

Pseudolipomas

Pseudolipoma is defined as an encapsulated lesion that contains degenerated fat, and this is all enveloped by a liver capsule. This tumor is thought to arise from a detached piece of an epiploic appendage that undergoes degenerative changes and then it becomes covered by a fibrous capsule before lodging in the peritoneal cavity (35). This lesion may become attached to the liver capsule when it is in close proximity to the liver. The differential diagnoses of this uncommon entity include serosal metastatic nodule, fibrosing subcapsular necrotic nodule and parasitic infections such as echinococcosis. On CT, it appears as a well-circumscribed nodule on the liver surface with a center of fat or soft-tissue attenuation. On the MR images, it appears as fat signal intensity on all the MRI sequences (1) (Fig. 12). Pseudolipoma does not require any treatment.

CONCLUSION

Identification of fat within an intraperitoneal or retroperitoneal lesion can help narrow the differential diagnosis. When such lesions are detected, their origin and

characteristic imaging features are critical for differentiating between lesions that need surgical resection and those that require medical treatment or no treatment at all (Fig. 13). Careful identification of the extent of the tumor is also important because incomplete resection can have an adverse effect upon the prognosis.

References

1. Prasad SR, Wang H, Rosas H, Menias CO, Narra VR, Middleton WD, et al. Fat-containing lesions of the liver: radiologic-pathologic correlation. *Radiographics* 2005;25:321-331
2. Pereira JM, Sirlin CB, Pinto PS, Casola G. CT and MR imaging of extrahepatic fatty masses of the abdomen and pelvis: techniques, diagnosis, differential diagnosis, and pitfalls. *Radiographics* 2005;25:69-85
3. Israel GM, Bosniak MA, Slywotzky CM, Rosen RJ. CT differentiation of large exophytic renal angiomyolipomas and perirenal liposarcomas. *AJR Am J Roentgenol* 2002;179:769-773
4. Singer S, Antonescu CR, Riedel E, Brennan MF. Histologic subtype and margin of resection predict pattern of recurrence and survival for retroperitoneal liposarcoma. *Ann Surg* 2003;238:358-370
5. Weiss SW. *Lipomatous tumors*. In: Weiss SW, Brooks JSJ, eds. *Soft tissue tumors*. Baltimore: Williams & Wilkins, 1996:207-251
6. Kim T, Murakami T, Oi H, Tsuda K, Matsushita M, Tomoda K, et al. CT and MR imaging of abdominal liposarcoma. *AJR Am J Roentgenol* 1996;166:829-833
7. Kawano R, Nishie A, Yoshimitsu K, Irie H, Tajima T, Hirakawa M, et al. Retroperitoneal well-differentiated inflammatory liposarcoma: a diagnostic dilemma. *Radiat Med* 2008;26:450-453
8. Dei Tos AP. Liposarcoma: new entities and evolving concepts. *Ann Diagn Pathol* 2000;4:252-266
9. Song T, Shen J, Liang BL, Mai WW, Li Y, Guo HC. Retroperitoneal liposarcoma: MR characteristics and pathological correlative analysis. *Abdom Imaging* 2007;32:668-674
10. Tateishi U, Hasegawa T, Beppu Y, Satake M, Moriyama N. Primary dedifferentiated liposarcoma of the retroperitoneum. Prognostic significance of computed tomography and magnetic resonance imaging features. *J Comput Assist Tomogr* 2003;27:799-804
11. Gatcombe HG, Assikis V, Kooby D, Johnstone PA. Primary retroperitoneal teratomas: a review of the literature. *J Surg Oncol* 2004;86:107-113
12. Taori K, Rathod J, Deshmukh A, Sheorain VS, Jawale R, Sanyal R, et al. Primary extragonadal retroperitoneal teratoma in an adult. *Br J Radiol* 2006;79:E120-E122
13. Davidson AJ, Hartman DS, Goldman SM. Mature teratoma of the retroperitoneum: radiologic, pathologic, and clinical correlation. *Radiology* 1989;172:421-425
14. Kurosaki Y, Tanaka YO, Itai Y. Well-differentiated liposarcoma of the retroperitoneum with a fat-fluid level: US, CT, and MR appearance. *Eur Radiol* 1998;8:474-475
15. Commons RR, Callaway CP. Adenomas of the adrenal cortex. *Arch Med Interna* 1948;81:37-41
16. Korobkin M, Giordano TJ, Brodeur FJ, Francis IR, Siegelman ES, Quint LE, et al. Adrenal adenomas: relationship between histologic lipid and CT and MR findings. *Radiology* 1996;200:743-747
17. L'Hostis H, Deminiere C, Ferriere JM, Coindre JM. Renal angiomyolipoma: a clinicopathologic, immunohistochemical, and follow-up study of 46 cases. *Am J Surg Pathol* 1999;23:1011-1020
18. Hajdu SI, Foote FW Jr. Angiomyolipoma of the kidney: report of 27 cases and review of the literature. *J Urol* 1969;102:396-401
19. Israel GM, Hindman N, Hecht E, Krinsky G. The use of opposed-phase chemical shift MRI in the diagnosis of renal angiomyolipomas. *AJR Am J Roentgenol* 2005;184:1868-1872
20. Wagner BJ, Wong-You-Cheong JJ, Davis CJ Jr. Adult renal hamartomas. *Radiographics* 1997;17:155-169
21. Schuster TG, Ferguson MR, Baker DE, Schaldenbrand JD, Solomon MH. Papillary renal cell carcinoma containing fat without calcification mimicking angiomyolipoma on CT. *AJR Am J Roentgenol* 2004;183:1402-1404
22. Kim JK, Park SY, Shon JH, Cho KS. Angiomyolipoma with minimal fat: differentiation from renal cell carcinoma at biphasic helical CT. *Radiology* 2004;230:677-684
23. Plaut A. Myelolipoma in the adrenal cortex; myeloadipose structures. *Am J Pathol* 1958;34:487-515
24. Kenney PJ, Wagner BJ, Rao P, Heffess CS. Myelolipoma: CT and pathologic features. *Radiology* 1998;208:87-95
25. Musante F, Derchi LE, Zappasodi F, Bazzocchi M, Riviezzo GC, Banderali A, et al. Myelolipoma of the adrenal gland: sonographic and CT features. *AJR Am J Roentgenol* 1988;151:961-964
26. Meyer A, Behrend M. Presentation and therapy of myelolipoma. *Int J Urol* 2005;12:239-243
27. Kumar M, Duerinckx AJ. Bilateral extraadrenal perirenal myelolipomas: an imaging challenge. *AJR Am J Roentgenol* 2004;183:833-836
28. Outwater EK, Siegelman ES, Hunt JL. Ovarian teratomas: tumor types and imaging characteristics. *Radiographics* 2001;21:475-490
29. Marina NM, Cushing B, Giller R, Cohen L, Lauer SJ, Ablin A, et al. Complete surgical excision is effective treatment for children with immature teratomas with or without malignant elements: A Pediatric Oncology Group/Children's Cancer Group Intergroup Study. *J Clin Oncol* 1999;17:2137-2143
30. Caspi B, Appelman Z, Rabinerson D, Zalel Y, Tulandi T, Shoham Z. The growth pattern of ovarian dermoid cysts: a prospective study in premenopausal and postmenopausal women. *Fertil Steril* 1997;68:501-505
31. Ayhan A, Bukulmez O, Genc C, Karamursel BS, Ayhan A. Mature cystic teratomas of the ovary: case series from one institution over 34 years. *Eur J Obstet Gynecol Reprod Biol* 2000;88:153-157
32. Daskalogiannaki M, Voloudaki A, Prassopoulos P, Magkanas E, Stefanaki K, Apostolaki E, et al. CT evaluation of mesenteric panniculitis: prevalence and associated diseases. *AJR Am J Roentgenol* 2000;174:427-431
33. Kikiros CS, Edis AJ. Mesenteric panniculitis resulting in bowel obstruction: response to steroids. *Aust N Z J Surg* 1989;59:287-290
34. Popkharitov AI, Chomov GN. Mesenteric panniculitis of the sigmoid colon: a case report and review of the literature. *J Med Case Reports* 2007;1:108
35. Quinn AM, Guzman-Hartman G. Pseudolipoma of Glisson capsule. *Arch Pathol Lab Med* 2003;127:503-504